ChemPubSoc Europe

DOI: 10.1002/cphc.201300677

Anomalous Property of $Ag(BO_2)_2$ Hyperhalogen: Does Spin–Orbit Coupling Matter?

Hui Chen,*[a] Xiang-Yu Kong,[b] Weijun Zheng,*[b] Jiannian Yao,[a] Anil K. Kandalam,[c] and Puru Jena[d]

Hyperhalogens were recently identified as a new class of highly electronagative species which are composed of metals and superhalogens. In this work, high-level theoretical calculations and photoelectron spectroscopy experiments are systematically conducted to investigate a series of coinage-metal-containing hyperhalogen anions, $Cu(BO_2)_2^-$, $Ag(BO_2)_2^-$, and $Au(BO_2)_2^-$. The vertical electron detachment energy (VDE) of $Ag(BO_2)_2^-$ is anomalously higher than those of $Au(BO_2)_2^-$ and $Cu(BO_2)_2^-$. In quantitative agreement with the experiment, high-level ab initio calculations reveal that spin–orbit coupling (SOC) lowers the VDE of $Au(BO_2)_2^-$ significantly. The sizable magnitude of about 0.5 eV of SOC effect on the VDE of $Au(BO_2)_2^-$ demonstrates that SOC plays an important role in the electronic structure of gold hyperhalogens. This study represents a new paradigm for relativistic electronic structure calculations for the one-electron-removal process of ionic Au^IL_2 complexes, which is characterized by a substantial SOC effect.

1. Introduction

The importance of negative ions in chemical industry as strong oxidizing agents has led to a constant search to find molecules/clusters whose electron affinities (EAs) can far exceed those of halogen atoms. Since the initial discovery[1,2] that PtF_6 can oxidize O_2 and Xe half a century ago, and that its EA of 7.0 eV[3] far exceeds that of Cl (3.61 eV), considerable progress has been made in the design and synthesis of superhalogens, first termed by Gutsev and Boldyrev.[4,5] Typical superhalogens reported in the literature can be represented by the formula MX_{k+1} or $MO_{(k+1)/2}$, where M is a main group or transition metal atom X is a halogen atom, and k is the maximal formal valence of the M atom.[6–9] Superhalogens can be metal-free,[10] halogen-free,[11] or both.[12] Theoretical predictions suggest that $H_{12}F_{13}$ can have an EA as high as 14 eV.[13] In a recent publication,[14] it has been shown that a new class of species, called hyperhalogens, can be synthesized, which are composed of a metal atom at the core surrounded by superhalogen moieties, much the same way as superhalogens are created by surrounding a metal atom with halogen atoms. The EAs of these hyperhalogens are even larger than those of their superhalogen building blocks, thus providing a pathway to create strong negative ions. This discovery was made while systematically studying the interactions of BO_2 with Au and finding that the EA of $Au(BO_2)_2$ was significantly larger than that of BO_2.[7] Subsequent experiments[15] on $Cu(BO_2)_2$ confirmed that this compound is also a hyperhalogen. A natural curiosity was then to see if $Ag(BO_2)_2$ exhibits the same behavior. While our present experiment confirms this to be the case, we found that the variation in EA with the metal atom of $M(BO_2)_2$ (M = Cu, Ag, and Au) is different to what has been reported for MF_2[16] and $M(CN)_2$ (M = Cu, Ag, Au).[17] The EAs of $M(BO_2)_2$ are 5.07, 6.20, and 5.7 eV for Cu, Ag, and Au, respectively. In contrast, the EAs of MF_2 and $M(CN)_2$ systematically increase with the metal atom. For example, the EAs of MF_2 (M = Cu, Ag, and Au) are 3.79, 4.76, and 4.84 eV, respectively, while it is 5.29, 6.06, and 6.09 eV for $Cu(CN)_2$, $Ag(CN)_2$, and $Au(CN)_2$.

This anomalous behavior of Ag is surprising as among the coinage metals it is Au that is known to exhibit anomalous properties. The ionization potential (IP) of Cu, Ag, and Au are 7.726, 7.576, and 9.226 eV, respectively, while their EAs are, 1.236, 1.304, and 2.309 eV.[18] The substantially enhanced IP and EA values of Au, as well as its many unique properties both in nanostructure and bulk form, are due to the relativistic effects and its aurophilic nature. The anomalous results for $Ag(BO_2)_2$ raises the question: Is it due to spin–orbit coupling or due to the a unique property of the superhalogen ligand?

In previous studies of $Au(BO_2)_2$ and $Cu(BO_2)_2$ systems, density functional theory (DFT) within scalar relativistic formulation has been used to calculate the molecular structures and vertical/

[a] Prof. Dr. H. Chen, Prof. Dr. J. N. Yao
Beijing National Laboratory for Molecular Sciences
CAS Key Laboratory of Photochemistry, Institute of Chemistry
Chinese Academy of Sciences (CAS)
Beijing 100190 (China)
E-mail: chenh@iccas.ac.cn

[b] X. Y. Kong, Prof. Dr. W. J. Zheng
State Key Laboratory of Molecular Reaction Dynamics
Institute of Chemistry, CAS, Beijing 100190 (China)
E-mail: zhengwj@iccas.ac.cn

[c] Prof. Dr. A. K. Kandalam
Department of Physics, West Chester University
West Chester, PA 19383 (USA)

[d] Prof. Dr. P. Jena
Department of Physics, Virginia Commonwealth University
Richmond, VA 23284 (USA)

Supporting information for this article is available on the WWW under http://dx.doi.org/10.1002/cphc.201300677.

adiabatic electron detachment energies (VDE/ADE) of the hyperhalogen anions (the ADE is equivalent to the EA as long as the structures of the neutral and the anion are not much different). To date, most studies have ignored a fundamentally important physical factor, spin-orbit coupling (SOC), which is a non-scalar relativistic effect. Owing to the linear dependence of the SOC effect on nuclear charge,[19] a non-negligible SOC effect is expected for very heavy transition metals such as Au. As shown in many high-level sophisticated ab initio multi-configurational calculations on the VDE/ADE of Au-containing systems, such as AuO^-,[20] AuO_2^-,[21] $Au(CN)_2^-$,[17] AuH_2^-,[22] AuI_2^-,[23,24] and $[XAu(CN)]^-$ (X = F, Cl, Br, and I),[25] consideration of SOC is essential to achieve quantitative agreement with the photoelectron spectroscopy (PES) experiments. No studies are available that include the SOC effect in coinage-metal-containing hyperhalogens such as $M(BO_2)_2$. More generally, to the best of our knowledge, previous high-level ab initio SOC studies for Au-containing systems never reported any results about the absolute magnitude of the SOC effect on the VDE or ADE values.[17,20–26]

Here we present our experimental results followed by a high-level theoretical study of $M(BO_2)_2$ (M = Cu, Ag, Au), which includes the SOC effect. We show that the anomalous result of $Ag(BO_2)_2$ is apparent at the CCSD(T) level of theory without inclusion of SOC. This implies that the interaction of superhalogens with coinage-metal atoms is indeed different from that of halogen atoms because of the increasing ability of the former to draw electrons from the metal atom. However, the SOC effect is needed for a quantitative interpretation of the experimental results. The results reported herein can thus directly provide an estimation of the SOC effect for related systems of future studies.

2. Results and Discussion

The measured photoelectron spectrum of $Ag(BO_2)_2^-$ is presented in Figure 1. It shows a sharp peak centered at ~6.28 eV. The experimental VDE/ADE of $Ag(BO_2)_2^-$ are determined to be 6.28/6.20 eV based on the photoelectron spectrum. These values are higher than those of $Cu(BO_2)_2^-$ (5.28/5.07 eV), measured previously by Feng et al.,[15] as well as those of $Au(BO_2)_2^-$ with VDE/ADE of (5.9/5.7 eV).[14] Thus, it is clear that $Ag(BO_2)_2$ is a hyperhalogen similar to $Au(BO_2)_2$ and $Cu(BO_2)_2$. But it is unclear why the VDE of $Ag(BO_2)_2^-$ is higher than that of $Au(BO_2)_2^-$. We sought the answer to this puzzle through ab initio and first-principles calculations at various levels of theory.

We begin with the geometries of hyperhalogen anions $Au(BO_2)_2^-$, $Ag(BO_2)_2^-$, and $Cu(BO_2)_2^-$ (Figure 2), which were optimized at the DFT level using the PBE0 functional. The Cartesian coordinates of these species are available in the Supporting Information. We note that the M–O bond distances in $Ag(BO_2)_2^-$ are the longest among the three species. A similar geometric trend has also been reported before in coinage-metal-containing complexes of MF_2^-, $M(CN)_2^-$, M(CN), and MI_2^-.[16,17,23,27–29] Thus, the result of a longer Ag-ligand bond length than its congeners is likely to be a common feature in coinage-metal species. The geometry of the BO_2^- ligand is

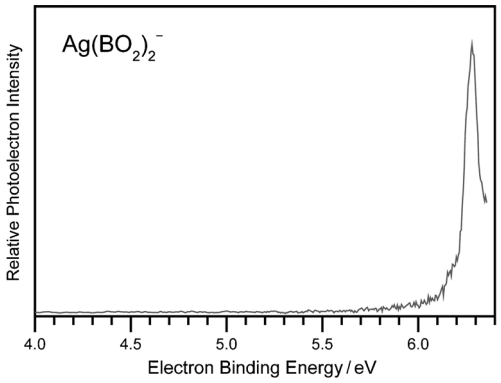

Figure 1. Photoelectron spectrum of $Ag(BO_2)_2^-$ recorded with 193 nm photons.

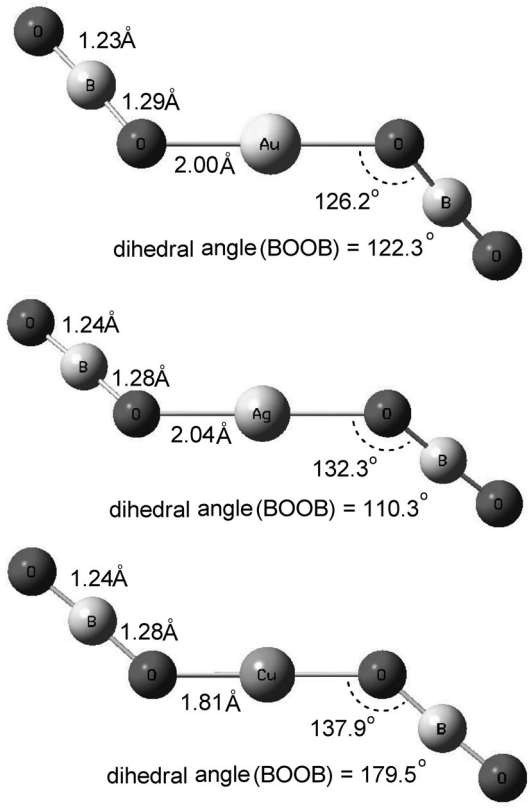

Figure 2. Optimized geometries of hyperhalogen anions $Au(BO_2)_2^-$, $Ag(BO_2)_2^-$, and $Cu(BO_2)_2^-$.

almost unchanged in all three species, indicating its integrity in bonding with the central metal atoms. $Cu(BO_2)_2^-$ is planar, while $Au(BO_2)_2^-$ and $Ag(BO_2)_2^-$ are not. Interestingly, the degree of non-planarity of these three molecules is in line with the trend of the M–O bond lengths, namely, $Ag(BO_2)_2^-$ being the extreme case; it has the most non-planar geometry among all three species.

We now study the SOC effect on the electronic structure of $Cu(BO_2)_2$, $Ag(BO_2)_2$, and $Au(BO_2)_2$. First, it is helpful to construct an electronic structure picture of the neutral hyperhalogens $M(BO_2)_2$ from their closed-shell anions. In Figure 3, we show the five high-lying doubly occupied valence-shell molecular or-

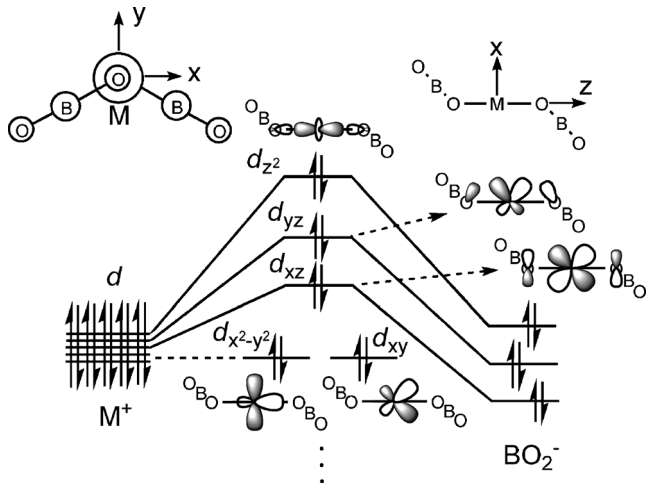

Figure 3. The high-lying MOs containing metal-valence d components in $M(BO_2)_2^-$ (if M = Au, d_{yz} is higher in energy than d_{z^2}).

bitals (MOs) of the $M(BO_2)_2$ anion, which are mainly composed of five d-atomic orbitals of the central metal atom. It can be seen that due to the interaction with the orbitals of two BO_2^- ligands, the otherwise degenerate metal d shell splits. When an electron is removed from the high-lying valence d shell of the hyperhalogen anion, five low-lying doublet ($S = 1/2$) electronic states can be generated in principle. Each of the states is characterized by the orbital from which the electron is removed, that is, by the location of the hole. The absence of strong Au-ligand covalent bonding character in $Au(BO_2)_2$ prevents the states from severe metal d-shell splitting, leading to low and close-lying electronic states. The proposed close-lying character of these five doublet states of neutral $M(BO_2)_2$ is confirmed by our CCSD(T)/CBS and MRCISD + Q calculations for all three complexes containing Cu, Ag, and Au at their anion equilibrium structures, which demonstrates that the three states of $^2D(d_{z^2}/d_{yz}/d_{xz}$, hole in $d_{z^2}/d_{yz}/d_{xz}$ orbitals) are close in energy (within 7 kcal mol^{-1}), while the other two states of $^2D(d_{xy}/d_{x^2-y^2}$, hole in $d_{xy}/d_{x^2-y^2}$ orbitals) are separated from these three states by about 20 kcal mol^{-1}. The $^2D(d_{xy})$ and $^2D(d_{x^2-y^2})$ states are almost degenerate because they are both nonbonding d orbitals which do not overlap with the BO_2^- ligand orbitals. The above electronic structure picture of low and close-lying states is the basis for the SOC effect.

Concerning the configurational identity of the lowest electronic state at the corresponding anion equilibrium geometry, we observed some qualitative difference between the gold complex and the two Ag and Cu complexes. For $Au(BO_2)_2$, the lowest state is $^2D(d_{yz})$, which is about 1.9 kcal mol^{-1} lower than $^2D(d_{z^2})$ at the CCSD(T)/CBS level. In contrast, for both $Ag(BO_2)_2$ and $Cu(BO_2)_2$ the lowest states are $^2D(d_{z^2})$, which are about 3.1 and 4.1 kcal mol^{-1} lower than $^2D(d_{yz})$ at the CCSD(T)/CBS level.

MRCI/CCSD(T)&MRCI + Q/SO level of theory was used to calculate the SOC effect. In this approach, the SOC was computed at the MRCI level including the aforementioned five doublet states, while the SO-free state energies were determined by CCSD(T)/CBS (for the two lowest states) and MRCI + Q (for the other three states) methods. The corresponding SOC computational results are collected in Table 1.

Table 1. Experimental and calculated VDE [eV] of the $M(BO_2)_2^-$ (M = Cu, Ag, Au) clusters.

Clusters	Theoretical CCSD(T)/CBS	SOC correction	CCSD(T)/CBS + SOC	Exptl[a]
$Au(BO_2)_2^-$	6.32	−0.45	5.87	5.9(1)[b]
$Ag(BO_2)_2^-$	6.50	−0.10	6.40	6.28(8)[c]
$Cu(BO_2)_2^-$	5.49	−0.04	5.45	5.28(8)[d]

[a] The numbers in parentheses indicate the experimental uncertainty in the last digits. [b] From ref. [14]. [c] This work. [d] From ref. [15].

First, it can be seen that our high-level coupled-cluster calculations with the SOC effect generate quantitatively accurate VDE values for $Au(BO_2)_2^-$, $Ag(BO_2)_2^-$, and $Cu(BO_2)_2^-$. For $Au(BO_2)_2^-$, the calculated VDE value of 5.87 eV is very close to the experimental value of 5.9 eV. For $Ag(BO_2)_2^-$ and $Cu(BO_2)_2^-$ the deviations from the experimental values are a little larger, around 0.12–0.17 eV. However, considering the experimental uncertainty of ±0.08 eV, the current theoretical results are in general good agreement with the experiment. It should be noted that the unusual experimental observation of $Ag(BO_2)_2^-$ having the highest VDE value among this series of coinage-metal species is confirmed by our computational results. Second, inspecting the magnitudes of the SOC effect, it can be seen that the order of relativistic effect in this series of coinage metals is consistent with the nuclear-charge-based intuition that the heavier the nucleus, the larger the SOC effect. Especially for the gold complex, its significant magnitude of 0.45 eV demonstrates that consideration of the SOC effect in VDE calculation is important. In a similar way, EA can also be affected by SOC. Although the SOC effects for silver and copper complexes are much smaller than that for the gold complex, the magnitude of 0.1 eV for the silver species can still be considered to be quantitatively meaningful. The SOC effect is small for copper species and can be safely omitted.

Through this series of SOC calculations, we determined the net SOC effect on the first VDE of these coinage-metal-containing hyperhalogens for the first time. Especially for $Au(BO_2)_2^-$, our results suggest that for such type of gold species, with close-lying electronic states, it is important to consider the SOC effect in electronic structure calculations in order to achieve quantitative agreement with the photoelectron spectroscopy experiments. It is noteworthy that for the one-electron reduction potentials of octahedral Os^{3+}/Ru^{3+} containing complexes SOC effect values of similar size (0.3/0.07 eV) as found herein for the Au/Ag pair have been reported previously.[30]

As mentioned above, the VDEs of the $M(CN)_2$ series reported by Wang et al.[17] increase systematically, with $Au(CN)_2$ having the highest VDE of 6.09 eV in the series, thereby obeying the periodic trend of group IB. A similar trend was also reported for the MF_2 series.[16] However, in the $M(BO_2)_2$ series, the order of the VDEs for $Au(BO_2)_2^-$ and $Ag(BO_2)_2^-$ is switched, and the VDEs are in the order of $Ag(BO_2)_2^- > Au(BO_2)_2^- > Cu(BO_2)_2^-$. Thus, it seems that $M(BO_2)_2$ clusters are special. The ligand BO_2

itself is a superhalogen with high EA, that is, it is a hard acid in the context of Lewis hard and soft acids and bases. BO_2 can withdraw charge from the metal atom more effectively than halogens can. This is corroborated by charge population results calculated by DFT for the central metal in the ML_2^- series (M = Cu, Ag, and Au; L = BO_2^-, F^-, and CN^-), as shown in Table 2. Hence, this series of $M(BO_2)_2$ species constitutes coinage-metal complexes that are characterized mainly by ionic metal–ligand bonding. It is this feature that distinguishes $M(BO_2)_2$ species from those possessing considerable covalent bonding character, such as AuO^-,[20,21] AuO_2^-,[21] $Au(CN)_2^-$,[17] AuH_2^-,[22] AuI_2,[23,24] and other systems.[16,25,26]

Table 2. DFT calculated charge populations from natural population analysis (NPA) for the ML_2^- series (M = Cu, Ag, Au; L = BO_2^-, F^-, $CN^{<M->}$).

M	NPA charge populations[a]		
	L = BO_2^-	L = F^-	L = CN^-
Au	0.545	0.481	0.190
Ag	0.744	0.677	0.333
Cu	0.707	0.638	0.325

[a] Calculated by the PBE0 functional using the ATZ basis set.

Without strong covalent Au–L bonding, the necessarily associated close-lying electronic states in $Au(BO_2)_2$, as revealed above, affect the first VDE of $Au(BO_2)_2^-$ by a large SOC effect. Such net effects of SOC on VDEs have never been reported before for other systems. If we attribute the difference between the experimental first VDE value and previously reported high-level CCSD(T) results to the SOC effect, we reach the conclusion that this SOC effect for the first VDE of $Au(BO_2)_2^-$ obtained herein is much larger than those from Au systems with a significant covalent bonding character.[17,20–25] This implies that SOC has a stronger effect on the VDE of Au species that are characterized by ionic bonding than those characterized by covalent bonding. This large SOC effect is mainly rooted in the close-lying electronic states. In the absence of these, the SOC effect is small as has been recently observed for heavy Pt and Ir metals.[31]

We also note in Table 1 that the anomaly in the VDE of $Ag(BO_2)_2$ among the coinage-metal systems is already apparent at the CCSD(T) level of theory. At this level the VDE of $Ag(BO_2)_2$ is 0.18 eV higher than that of $Au(BO_2)_2$. However, experimentally this difference is significantly larger, namely 0.38 eV. Including the SOC this difference is 0.53 eV, which agrees with the experiment within the experimental uncertainty.

3. Conclusions

In summary, we have systematically studied a series of coinage-metal-containing species of $Au(BO_2)_2$, $Ag(BO_2)_2$, and $Cu(BO_2)_2$. By combined experiments and ab initio quantum chemical calculations, we have shown that: 1) The VDE/ADE of $Ag(BO_2)_2^-$ are higher than those of the previously reported hyperhalogen anions $Au(BO_2)_2^-$ and $Cu(BO_2)_2^-$. This confirms that, $Ag(BO_2)_2$ is a hyperhalogen. 2) In contrast to the cases of Cu- and Ag-containing hyperhalogens, the SOC effect significantly lowers the electron detachment energy of Au-containing hyperhalogens. That explains why $Au(BO_2)_2^-$ unusually has a much lower VDE than $Ag(BO_2)_2^-$ does. 3) Although the anomaly in the VDE of $Ag(BO_2)_2$ is apparent at the CCSD(T) level of theory, the SOC effect has to be taken into account to achieve quantitative agreement. 4) The SOC magnitude of around 0.5 eV determined herein for the first time clearly demonstrates that SOC is important in electronic structure calculations. This study reveals a new paradigm for electronic structure calculations for relativistic systems. Based on the result of $Au(BO_2)_2$, we suspect that such a substantial SOC effect is most likely to be common in one-electron-removal processes of bicoordinated Au^IL_2 complexes, for which there is no strong covalent Au–L bonding present. The universality of this interesting conjecture awaits more computational investigations in the future.

Experimental and Computational Section

Experiments were conducted in a home-built apparatus consisting of a time-of-flight mass spectrometer and a magnetic-bottle photoelectron spectrometer, which have been described elsewhere.[32] Briefly, the $Ag(BO_2)_2^-$ cluster was produced in a laser vaporization source by ablating a rotating, translating $Ag/Ag_2O/B$ mixture target (13 mm diameter, $Ag/Ag_2O/B$ mole ratio 5:1:1) with the second harmonic (532 nm) light pulses of a Nd:YAG laser, while helium gas with 4 atm backing pressure was allowed to expand through a pulsed valve over the target. The typical laser power used in this work was ~10 mJ·pulse^{-1}. The cluster anions were mass-analyzed by the time-of-flight mass spectrometer. The $Ag(BO_2)_2^-$ cluster was mass-selected and decelerated before being photodetached with 193 nm (6.424 eV) photons (0.1–0.2 mJ pulse^{-1}). The resulting electrons were energy-analyzed by the magnetic-bottle photoelectron spectrometer. The PES spectra were calibrated using the spectra of Cu^- and Ag^- taken under similar conditions. The instrumental resolution was approximately 40 meV for electrons with 1 eV kinetic energy.

The equilibrium structures of the hyperhalogen anions were first optimized with DFT. Due to its good performance in geometry optimization, found from previous calibration studies on coinage-metal-containing systems,[33–35] the PBE0[36,37] hybrid functional was used, combined with the aug-cc-pVTZ-PP[38] and aug-cc-pVTZ[39] basis sets (denoted as ATZ in this work) of augmented multiply polarized triple-ζ quality for metals and main-group elements, respectively. To account for the scalar relativistic effect, the new MCDHF pseudopotentials (PPs)[40] for coinage metals were employed in all our calculations. Geometry optimizations were done without any symmetry constraints. The true energy-minimum character of the optimized structures was verified by harmonic vibrational analysis, which showed no imaginary frequencies. Natural population analysis (NPA) charges[41] were calculated by PBE0 with the ATZ basis set. All DFT calculations were performed with the Gaussian 09 program.[42]

The ab initio wave function theory (WFT) calculations employing high-level coupled-cluster (CCSD(T))[43] and multireference configuration interaction (MRCI)[44] methods based on DFT-optimized structures were all performed with the MOLPRO package.[45] In all ab initio calculations, the atomic inner shell core electrons were not correlated. The SOC effect was included using a contracted SO config-

uration interaction method[46] with two-component spin-orbit (SO) PPs[40] on coinage metals. Five electronic states were included in the SOC state-interacting calculations. The SOC matrix was constructed on a basis of the MRCI state-specific scalar relativistic states. The MRCI calculations for the SOC matrix used ATZ basis sets. The matrix was then diagonalized to obtain the SO states and energies. For a more accurate determination of the state-specific scalar relativistic energies of all states, we calculated the relative energies of the higher four states compared to the lowest state by the CCSD(T)/CBS method (for the second state) and the MRCI+Q/ATZ method (including Davidson's cluster correction "+Q", for the third, fourth, and fifth states). The diagonal elements of SOC matrix were then replaced by the individual state energies generated from the above relative energies to the ground state. In this work we termed this combined approach as MRCI/CCSD(T)&MRCI+Q/SO. The two-point complete basis set (CBS) limit extrapolation of CCSD(T) total electronic energy was done based on the ADZ-ATZ basis set pair, employing the formula of $E_{total,n} = E_{total,CBS} + A/(n+1/2)^4$,[47] wherein n is the cardinal number of the basis sets ($n = 2$, 3 for ADZ, ATZ). This formula was found to perform better than the alternatives.[48] To improve the reliability of CCSD(T) method, following our previous practices,[49–51] DFT Kohn–Sham orbitals of the PBE0 functional rather than Hartree–Fock orbitals were used as reference. The active space of the preceding CASSCF calculations for all our MRCI calculations is composed of five d orbitals of central transition metals. Different from the often used CASSCF method, the MRCI method employed for the SOC effect in this work includes not only non-dynamic but also dynamic electron correlation, which enabled us to use a relatively small active space.

Acknowledgements

This work was supported by the National Science Foundation of China (Nos. 21290194 and 21273246), the Chinese Academy of Sciences, and the U.S. Department of Energy, Office of Basic Energy Sciences, Division of Materials Sciences and Engineering under Award # DE-FG02-96ER45579.

Keywords: ab initio calculation · coinage metals · hyperhalogen · photoelectron spectroscopy · spin–orbit coupling

[1] N. Barttlett, *Proc. Chem. Soc.* **1962**, 218–218.
[2] N. Bartlett, D. H. Lohman, *Proc. Chem. Soc.* **1962**, 115–116.
[3] M. V. Korobov, S. V. Kuznetsov, L. N. Sidorov, V. A. Shipachev, V. N. Mit'kin, *Int. J. Mass Spectrom. Ion Processes* **1989**, *87*, 13–27.
[4] G. L. Gutsev, A. I. Boldyrev, *Chem. Phys.* **1981**, *56*, 277–283.
[5] G. L. Gutsev, A. I. Boldyrev, *Chem. Phys. Lett.* **1984**, *108*, 255–258.
[6] X.-B. Wang, C.-F. Ding, L.-S. Wang, A. I. Boldyrev, J. Simons, *J. Chem. Phys.* **1999**, *110*, 4763–4771.
[7] H. J. Zhai, L. M. Wang, S. D. Li, L.-S. Wang, *J. Phys. Chem. A* **2007**, *111*, 1030–1035.
[8] C. Sikorska, P. Skurski, *Inorg. Chem.* **2011**, *50*, 6384–6391.
[9] M. Marchaj, S. Freza, O. Rybacka, P. Skurski, *Chem. Phys. Lett.* **2013**, *574*, 13–17.
[10] G. L. Gutsev, P. Jena, R. J. Bartlett, *Chem. Phys. Lett.* **1998**, *292*, 289–294.
[11] G. L. Gutsev, R. K. Rao, P. Jena, X. B. Wang, L. S. Wang, *Chem. Phys. Lett.* **1999**, *312*, 598–605.
[12] B. Pathak, D. Samanta, R. Ahuja, P. Jena, *ChemPhysChem* **2011**, *12*, 2423–2428.
[13] S. Freza, P. Skurski, *Chem. Phys. Lett.* **2010**, *487*, 19–23.
[14] M. Willis, M. Götz, A. K. Kandalam, G. F. Ganteför, P. Jena, *Angew. Chem.* **2010**, *122*, 9150–9154; *Angew. Chem. Int. Ed.* **2010**, *49*, 8966–8970.
[15] Y. Feng, H.-G. Xu, W. J. Zheng, H. M. Zhao, A. K. Kandalam, P. Jena, *J. Chem. Phys.* **2011**, *134*, 094309.
[16] P. Koirala, M. Willis, B. Kiran, A. K. Kandalam, P. Jena, *J. Phys. Chem. C* **2010**, *114*, 16018–16024.
[17] X.-B. Wang, Y.-L. Wang, J. Yang, X.-P. Xing, J, Li, L.-S. Wang, *J. Am. Chem. Soc.* **2009**, *131*, 16368–16370.
[18] T. Andersen, H. K. Haugen, H. Hotop, *J. Phys. Chem. Ref. Data* **1999**, *28*, 1511–1533.
[19] M. Reiher, A. Wolf, *Relativistic Quantum Chemistry, the Fundamental Theory of Molecular Science*, Wiley-VCH, Weinheim, **2009**.
[20] T. Ichino, A. J. Gianola, D. H. Andrews, W. C. Lineberger, *J. Phys. Chem. A* **2004**, *108*, 11307–11313.
[21] H. J. Zhai, C. Burgel, V. Bonacic-Koutecky, L.-S. Wang, *J. Am. Chem. Soc.* **2008**, *130*, 9156–9167.
[22] H.-T. Liu, Y.-L. Wang, X.-G. Xiong, P. D. Dau, Z. A. Piazza, D.-L. Huang, C.-Q. Xu, J. Li, L.-S. Wang, *Chem. Sci.* **2012**, *3*, 3286–3295.
[23] Y.-L. Wang, X. B. Wang, X.-P. Xing, F. Wei, J. Li, L.-S. Wang, *J. Phys. Chem. A* **2010**, *114*, 11244–11251.
[24] S. Mishra, V. Vallet, W. Domcke, *ChemPhysChem* **2006**, *7*, 723–727.
[25] H.-T. Liu, X.-G. Xiong, P. D. Dau, Y.-L. Wang, J. Li, L.-S. Wang, *Chem. Sci.* **2011**, *2*, 2101–2108.
[26] Y.-L. Wang, H.-J. Zhai, L. Xu, J. Li, L.-S. Wang, *J. Phys. Chem. A* **2010**, *114*, 1247–1254.
[27] P. Zaleski-Ejgierd, M. Patzschke, P. Pyykkö, *J. Chem. Phys.* **2008**, *128*, 224303.
[28] O. Dietz, V. M. Rayón, G. Frenking, *Inorg. Chem.* **2003**, *42*, 4977–4984.
[29] M. Iliaš, P. Furdik, M. Urban, *J. Phys. Chem. A* **1998**, *102*, 5263–5268.
[30] M. Srnec, J. Chalupský, M. Fojta, L. Zendlová, L. Havran, M. Hocek, M. Kývala, L. Rulíšek, *J. Am. Chem. Soc.* **2008**, *130*, 10947–10954.
[31] K. J. Chen, G. L. Zhang, H. Chen, J. N. Yao, D. Danovich, S. Shaik, *J. Chem. Theory Comput.* **2012**, *8*, 1641–1645.
[32] H.-G. Xu, Z.-G. Zhang, Y. Feng, J. Y. Yuan, Y. C. Zhao, W. J. Zheng, *Chem. Phys. Lett.* **2010**, *487*, 204–208.
[33] R. H. Kang, H. Chen, S. Shaik, J. N. Yao, *J. Chem. Theory Comput.* **2011**, *7*, 4002–4011.
[34] M. Bühl, C. Reimann, D. A. Pantazis, T. Bredow, F. Neese, *J. Chem. Theory Comput.* **2008**, *4*, 1449–1459.
[35] S. Zhao, Z. H. Li, W. N. Wang, Z. P. Liu, K. N. Fan, Y. M. Xie, H. F. Schaefer, *J. Chem. Phys.* **2006**, *124*, 184102.
[36] J. P. Perdew, K. Burke, M. Ernzerhof, *Phys. Rev. Lett.* **1996**, *77*, 3865–3868.
[37] C. Adamo, V. Barone, *J. Chem. Phys.* **1999**, *110*, 6158–6170.
[38] K. A. Peterson, C. Puzzarini, *Theor. Chem. Acc.* **2005**, *114*, 283–296.
[39] T. H. Dunning, Jr., *J. Chem. Phys.* **1989**, *90*, 1007–1023.
[40] D. Figgen, G. Rauhut, M. Dolg, H. Stoll, *Chem. Phys.* **2005**, *311*, 227–244.
[41] A. E. Reed, R. B. Weinstock, F. Weinhold, *J. Chem. Phys.* **1985**, *83*, 735–746.
[42] Gaussian 09 (Revision A.02), M. J. Frisch, G. W. Trucks, H. B. Schlegel, G. E. Scuseria, M. A. Robb, J. R. Cheeseman, G. Scalmani, V. Barone, B. Mennucci, G. A. Petersson, H. Nakatsuji, M. Caricato, X. Li, H. P. Hratchian, A. F. Izmaylov, J. Bloino, G. Zheng, J. L. Sonnenberg, M. Hada, M. Ehara, K. Toyota, R. Fukuda, J. Hasegawa, M. Ishida, T. Nakajima, Y. Honda, O. Kitao, H. Nakai, T. Vreven, J. A. Montgomery, Jr., J. E. Peralta, F. Ogliaro, M. Bearpark, J. J. Heyd, E. Brothers, K. N. Kudin, V. N. Staroverov, R. Kobayashi, J. Normand, K. Raghavachari, A. Rendell, J. C. Burant, S. S. Iyengar, J. Tomasi, M. Cossi, N. Rega, J. M. Millam, M. Klene, J. E. Knox, J. B. Cross, V. Bakken, C. Adamo, J. Jaramillo, R. Gomperts, R. E. Stratmann, O. Yazyev, A. J. Austin, R. Cammi, C. Pomelli, J. W. Ochterski, R. L. Martin, K. Morokuma, V. G. Zakrzewski, G. A. Voth, P. Salvador, J. J. Dannenberg, S. Dapprich, A. D. Daniels, Ö. Farkas, J. B. Foresman, J. V. Ortiz, J. Cioslowski, D. J. Fox, Gaussian, Inc., Wallingford CT, **2009**.
[43] P. J. Knowles, C. Hampel, H.-J. Werner, *J. Chem. Phys.* **1993**, *99*, 5219–5227.
[44] H. J. Werner, P. J. Knowles, *J. Chem. Phys.* **1988**, *89*, 5803–5814.
[45] MOLPRO, version 2010.1, a package of ab initio programs, H.-J. Werner, P. J. Knowles, F. R. Manby, M. Schütz, P. Celani, G. Knizia, T. Korona, R. Lindh, A. Mitrushenkov, G. Rauhut, T. B. Adler, R. D. Amos, A. Bernhardsson, A. Berning, D. L. Cooper, M. J. O. Deegan, A. J. Dobbyn, F. Eckert, E. Goll, C. Hampel, A. Hesselmann, G. Hetzer, T. Hrenar, G. Jansen, C.

Köppl, Y. Liu, A. W. Lloyd, R. A. Mata, A. J. May, S. J. McNicholas, W. Meyer, M. E. Mura, A. Nicklass, P. Palmieri, K. Pflüger, R. Pitzer, M. Reiher, T. Shiozaki, H. Stoll, A. J. Stone, R. Tarroni, T. Thorsteinsson, M. Wang, A. Wolf, see http://www.molpro.net.
[46] A. Berning, M. Schweizer, H.-J. Werner, P. J. Knowles, P. Palmieri, *Mol. Phys.* **2000**, *98*, 1823 – 1833.
[47] J. M. L. Martin, *Chem. Phys. Lett.* **1996**, *259*, 669 – 678.
[48] D. Feller, K. A. Peterson, J. G. Hill, *J. Chem. Phys.* **2011**, *135*, 044102.
[49] H. Chen, K. B. Cho, W. Z. Lai, W. Nam, S. Shaik, *J. Chem. Theory Comput.* **2012**, *8*, 915 – 926.
[50] H. Chen, W. Z. Lai, J. N. Yao, S. Shaik, *J. Chem. Theory Comput.* **2011**, *7*, 3049 – 3053.
[51] H. Chen, W. Z. Lai, S. Shaik, *J. Phys. Chem. Lett.* **2010**, *1*, 1533 – 1540.

Received: July 23, 2013
Published online on August 13, 2013